How snowpack heterogeneity affects diurnal streamflow timing

Jessica D. Lundquist[1]
Scripps Institution of Oceanography, La Jolla, California, USA

Michael D. Dettinger[2]
U.S. Geological Survey, La Jolla, California, USA

Received 15 September 2004; revised 25 January 2005; accepted 4 February 2005; published 6 May 2005.

[1] Diurnal cycles of streamflow in snow-fed rivers can be used to infer the average time a water parcel spends in transit from the top of the snowpack to a stream gauge in the river channel. This travel time, which is measured as the difference between the hour of peak snowmelt in the afternoon and the hour of maximum discharge each day, ranges from a few hours to almost a full day later. Travel times increase with longer percolation times through deeper snowpacks, and prior studies of small basins have related the timing of a stream's diurnal peak to the amount of snow stored in a basin. However, in many larger basins the time of peak flow is nearly constant during the first half of the melt season, with little or no variation between years. This apparent self-organization at larger scales can be reproduced by employing heterogeneous observations of snow depths and melt rates in a model that couples porous medium flow through an evolving snowpack with free surface flow in a channel.

Citation: Lundquist, J. D., and M. D. Dettinger (2005), How snowpack heterogeneity affects diurnal streamflow timing, *Water Resour. Res.*, *41*, W05007, doi:10.1029/2004WR003649.

1. Introduction

[2] The time water takes to travel from the snow surface to the stream gauge is a measure of several key processes that operate in snowpacks and streams. For a given parcel of snowmelt, travel time through a basin equals the distance traveled divided by travel velocity, summed along segments of flow paths from melting to measurement. The distance traveled to a gauge depends on (1) the distance through the snow, (2) the distance traveled from the base of the snowpack to the channel, and (3) the distance through the river channel network. Along each flow path, travel velocities vary with location and increase with increasing discharge. Thus, by unraveling these various influences, timing can provide important new insights into basin-scale hydrology, including information about the rate of snowmelt, the location of snowmelt, the average depth of the snowpack, soil properties, average channel velocities, and the variability of snowpack properties across a basin.

[3] Predicting the travel times of runoff through river basins is essential for flood forecasting, and knowing the time of day of peak discharge can help hydropower plant operators maximize power production. For forecasting the time of peak discharge, streamflow output is the bottom line, and understanding the mean travel time through the basin is more important than that along any individual travel path. Diurnal cycles in streamflow provide a relatively unexplored method for determining these mean travel times. The hour of maximum discharge each day measures mean travel time through the basin, representing the time from peak melt (usually in early afternoon) to the time most water reaches the gauge. Diurnal cycles in streamflow have been observed in numerous high-altitude basins and at routinely monitored USGS gauges across the Western United States [*Lundquist and Cayan*, 2002]. Streamflow timing can be easily estimated from a pressure sensor without the necessity of a rating curve, allowing it to be studied without the need for the expense and intrusion of a complete gaging station.

[4] Textbooks, numerical models of the percolation of melted water through a snowpack, and observations of discharge from small basins all report that runoff travel times decrease as the snowpack thins and matures, reflecting shorter distances from the snow surface to the base of the snowpack [*Akan*, 1984; *Bengtsson*, 1981; *Braun and Slaymaker*, 1981; *Caine*, 1992; *Colbeck*, 1972; *Davar*, 1970; *Dunne et al.*, 1976; *Jordan*, 1983a, 1983b; *Kobayashi and Motoyama*, 1985; *Singh and Singh*, 2001; *Woo and Slaymaker*, 1975]. *Caine* [1992] and *Jordan* [1983a] both report decreases in daily travel times of about 1 hour per week during rapid snowmelt periods, while *Kobayashi and Motoyama* [1985] report daily runoff travel times that decrease 1.5 to 4 hours with each 1 m decrease in snow depth. These studies suggest that diurnal streamflow timing could be used to estimate snow water storage (SWS) in a basin.

[5] The correlation between diurnal streamflow timing and SWS is well illustrated in the Marble Fork of the Kaweah River (a 19 km^2 basin in Sequoia National Park, California, Figure 1a). Here, SWS is measured as the total amount of snow water that runs off past the gauge from a given date until the end of the melt season. In the Sierra

[1]Now at Climate Diagnostics Center, Cooperative Institute for Research in Environmental Sciences, Boulder, Colorado, USA.
[2]Also at Scripps Institution of Oceanography, La Jolla, California, USA.

0043-1397/05/2004WR003649$09.00

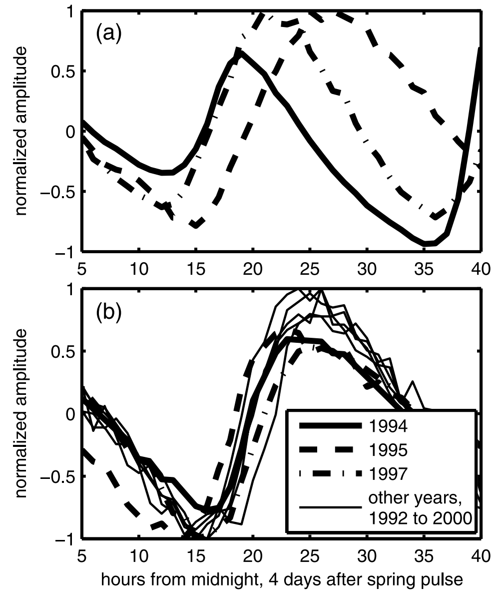

Figure 1. (a) Hourly streamflow timing at the Marble Fork of the Kaweah River (19 km^2 area, 2621 m elevation), Sequoia National Park, 4 days after the spring pulse. The spring pulse is defined as the day the river starts rising with spring melt [*Lundquist et al.*, 2004]. (b) Same as Figure 1a, for the Merced River at Happy Isles (469 km^2 area, 1224 m elevation), Yosemite National Park.

Nevada, little or no rain occurs during this period, so almost all discharge originates from snow. This method underestimates the actual SWS because of water losses from direct evaporation from the snowpack and transpiration through the trees. However, the estimated SWS is indicative of mean snow depth in a basin. At the Marble Fork gauge, the hour of peak streamflow covaries with the depth of the snowpack. In 1995, just after the onset of rapid snowmelt, the basin had 1652 mm SWS. At this time, peak flow occurred at 1:00 am, six hours later than in 1994, which had only 494 mm SWS (Figure 1a). In 1997, with 933 mm SWS, streamflow peaked at 9:00 pm. The time of diurnal peak flow shifted earlier within each year as the snowpack thinned (Figure 2a), and the hour of peak flow correlates well (r = 0.87) with the SWS in the basin (Figure 2b).

[6] However, most USGS gauges monitor watersheds larger than those that have been examined in these previous studies, and most gauges are located downstream, at elevations well below the snowfields. In the Merced River at Happy Isles (a 469 km^2 basin in Yosemite National Park, California, Figure 1b), streamflow following the onset of spring melt peaks at the same time of day each year, around 1:00 am, regardless of the amount of snow in the basin. Thus, at this basin scale, streamflow timing does not covary with snowpack depth. Indeed, during the peak melt season, the diurnal cycles of most USGS-gauged rivers in the western United States behave like the Merced River, with clear diurnal cycles but little or no change in the hour of peak flow as snowmelt progresses [*Lundquist and Cayan*, 2002, Figure 11a]. How does this consistency between years come about?

[7] One explanation for the differences in the evolution of diurnal cycles between the Marble Fork and Merced Rivers (and many others) could be that, in a larger basin, a greater fraction of travel time is spent in the channel, so that channel properties might establish these timing differences. However, average streamflow velocities in channels are fast compared to velocities in the snowpack, and in-channel velocities increase with discharge [*Rickenmann*, 1994]. Thus, as spring snowmelt and discharge rates increase, faster channel velocities would suggest shorter travel times and earlier peak flows, which are not observed in most larger basins. Alternatively, many larger basins span wide ranges of elevations, and travel distances and times in the channel presumably increase as the snow lines retreat to higher elevations. However, the snow line location and rate of retreat vary considerably between years and basins. The precise balances between the rates of snow line retreat and the SWS decline necessary to prevent overall travel time changes in so many larger basins seems implausible.

[8] Instead, this study proposes that variations in the evolution of diurnal timing with basin scale are products of the increasing heterogeneity in snowpack properties, particularly snow depths and melt rates, as larger and larger basins are considered. The magnitude and timing of snowmelt runoff and land surface climatic feedbacks depend on this same spatial heterogeneity [*Anderton et al.*, 2002; *Blöschl and Sivapalan*, 1995; *Giorgi and Avissar*, 1997; *Liston*, 1999; *Luce et al.*, 1998, 1999], and thus any insights

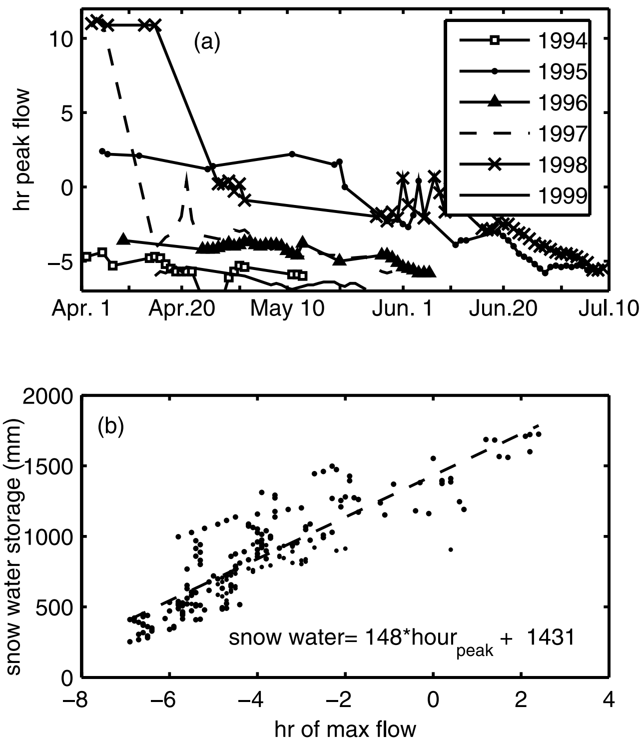

Figure 2. (a) Hour of peak flow (0 indicates midnight) over the course of the melt season in the Marble Fork of the Kaweah River. Periods with lines but no symbols indicate times when the stream's diurnal cycle timing was not clear because of cooling or spring storms. (b) Scatterplot of hour of peak flow versus snow water stored in the basin. Dashed line indicates potential predictive relationship between streamflow timing and the water stored in the basin, based on a least squares fit. Correlation coefficient is 0.87.

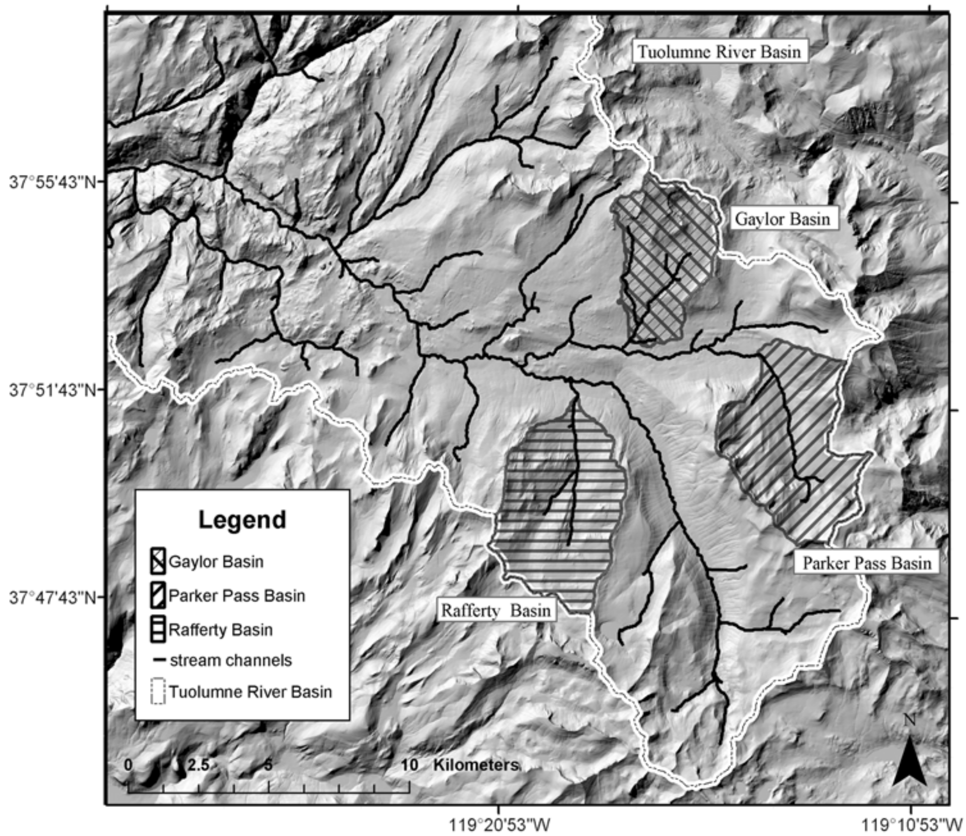

Figure 3. Map of three subbasins in the Tuolumne River watershed with different aspects and orientations in relationship to the primary storm track, which is from the west.

that the evolution of diurnal flow cycles can provide regarding heterogeneity are of interest. Spatial variability in snow water equivalent (SWE) has been observed on the order of 10–100 m [*Anderton et al.*, 2002], and this variability results in changes in snow covered area (SCA) as the shallowest deposits of snow disappear first from the landscape. Variations in SCA lead to significant variations in surface fluxes, energy advection, and the rate of snowpack depletion [*Anderton et al.*, 2002; *Shook and Gray*, 1997; *Williams et al.*, 1999].

[9] The current study tests the hypothesis that basin-scale-dependent heterogeneity of snowpack properties results in the observed changes in diurnal cycle timing with basin scale. First, observations are reviewed to show that much variation exists in measured snow depths and melt rates, and that subbasins within a river network can exhibit very different times of diurnal peaks (section 2). Second, a numerical model is developed (section 3). The model demonstrates that changing channel lengths have very little effect on diurnal streamflow timing, but changing heterogeneity of snow depths has a great effect (section 4). This study focuses on streamflow timing during the first half of the melt season, from the spring pulse (when the snowpack becomes ripe and discharge starts rising rapidly) to the date of peak flow (roughly when basin discharge is controlled more by decreases in snow covered area than by increases in temperature and solar insolation). During the first half of the season, snowmelt processes control streamflow timing, and most of the basin is consistently covered with snow. Later in the season, most snowmelt originates from the highest reaches of the basin, and diurnal streamflow timing depends on local patterns of SCA more than on basin scale.

2. Observations: Snowpack Heterogeneity

[10] Snowpack thickness, ripeness, and water content vary considerably within river basins, due to differing topographic settings, vegetation cover, and micrometeorological conditions [*Erxleben et al.*, 2002]. These snowpack differences can result in large differences in diurnal streamflow peaks in neighboring basins. The effect of heterogeneity on streamflow timing was examined for three subbasins of the Tuolumne River in Yosemite National Park, California. These basins are similar in size (16–25 km^2) but have different aspects and different orientations in relation to the primary winter storm track over the region, yielding different snow accumulation patterns (Figure 3). The Gaylor Creek Basin is oriented with its headwaters along the Sierra Crest, where winter storms originating from the Pacific Ocean drop large amounts of precipitation. Peak discharge from Gaylor Creek is delayed about 17 hours or more after the maximum snowmelt the previous afternoon, with a diurnal peak occurring at about 9:00 AM (Figure 4). This long delay reflects deep snowpacks and long travel times. In contrast, peak discharges from Parker Pass Creek and Rafferty Creek vary from 8:00 PM to midnight. Thus the time of peak discharge from nearby basins can differ by as much as 12 hours (Figure 4). The sum of the three flows, part of the input to the Tuolumne River downstream, is often semidiurnal and does not have a clear diurnal peak,

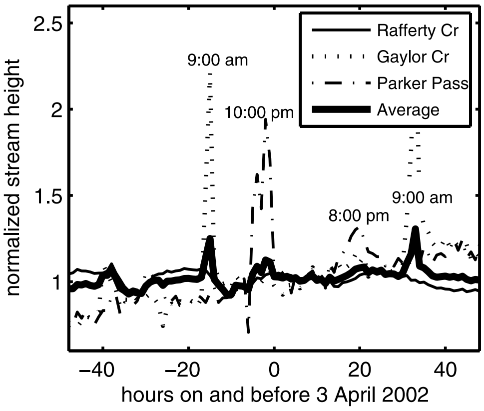

Figure 4. Normalized hourly stream depth versus time at three Tuolumne River subbasins, in Yosemite, California, for 2–3 April 2002. Thick solid line represents the average of the three and does not have a clear time of diurnal peak flow.

making it hard to distinguish the travel time signal from any individual basin.

[11] In order to develop a model to test the hypothesis that heterogeneity in snowpack properties is responsible for the observed changes in streamflow timing with basin scale (section 1), we need a quantitative measure of the mean and standard deviation of snowpack properties, as well as an estimate of how these properties change with basin scale. Snow pillows can be used to estimate the mean and standard deviation of three snow properties: snow water equivalent (SWE), melt rate, and snow depth. As an index of snow variability in western mountains, daily SWE measurements from 47 snow pillows at elevations from 1500 to 3000 m in the central Sierra Nevada, California (Figure 5, described further by *Lundquist et al.* [2004]) were compared. Daily differences in SWE measure the amount of water that leaves the snowpack weighed by the snow pillow. These differences were used to estimate the daily melt rates. Snow depth and SWE are measured simultaneously at 3 snow pillows (Gin Flat, Tuolumne Meadows, and Dana Meadows) in Yosemite National Park, so that their ratio provides a continuous record of snow density. Near the first of each month each spring, snow depth and density are manually sampled at snow courses throughout the Sierra. At snow pillows without direct measurements of snow depth, snow depth can be estimated from SWE by dividing by the average density observed at nearby snow courses.

[12] Using snow pillow data from 2003 as an example (Figure 6), initial snow depth can vary as much as 2 m between stations. The standard deviation, σ, is about 1 m, which is comparable with the average change in snow depth during the melt season. In 2003, average snow depth decreased about 1 m over 20 days, for an average melt rate of 5 cm d^{-1} and a standard deviation of about 1.5 cm d^{-1}. Because snow pillows are all located in flat, open spaces, actual variations due to different vegetative cover, slopes and aspects likely exceed those reported here. Thus the standard deviation of snow pillow SWE is a conservative estimate of true heterogeneity.

[13] During the melt season, when ripening of the snowpack leads to less variation in density, density varies less than depth in alpine areas [*Adams*, 1976; *Anderton et al.*, 2002; *Elder et al.*, 1991; *Logan*, 1973; *Shook and Gray*, 1997]. For example, SWE, depth and density were measured at 92 snow courses in the central Sierra Nevada near 1 May 2003. At this time, the mean SWE was 0.67 m $\pm$ 48%, and the mean depth was 1.58 m $\pm$ 48%. In contrast, the mean density, 430 kg m^{-3}, had a standard deviation of only $\pm$ 7%. Thus snow depth variations are the major source of SWE variation, and we estimated depth variations from SWE variations (which are more routinely measured) using a mean value for the density of ripened snow.

[14] The ranges of the properties of snowpacks contributing to streamflow increase at greater basin scales, particularly where the larger basins span wide ranges of elevations. Many operational snowmelt models assume linear relationships between elevation and snow depth [*Martinec*, 1987; *U.S. Army Corps of Engineers*, 1956],

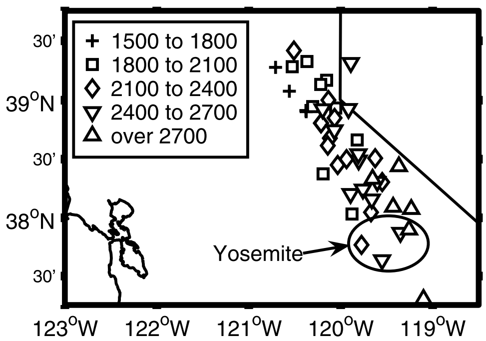

Figure 5. Locations of snow pillows examined in this study, labeled according to elevation. Snow pillows located within Yosemite National Park have been circled. Sequoia National Park is outside of the map boundaries, to the southeast.

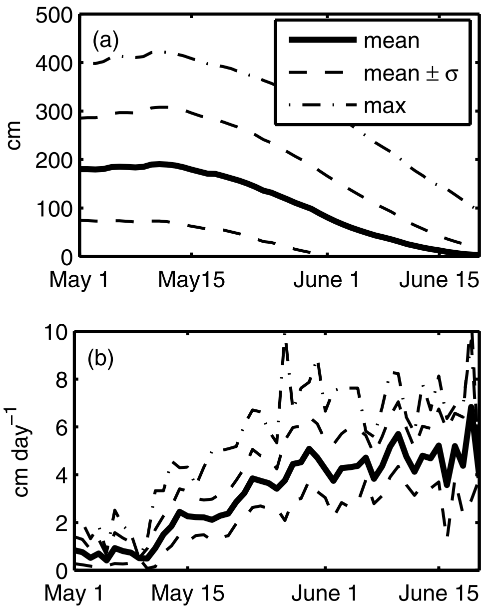

Figure 6. Average and standard deviation, σ, of (a) snow depth and (b) melt rate from central Sierra snow pillows for spring 2003.

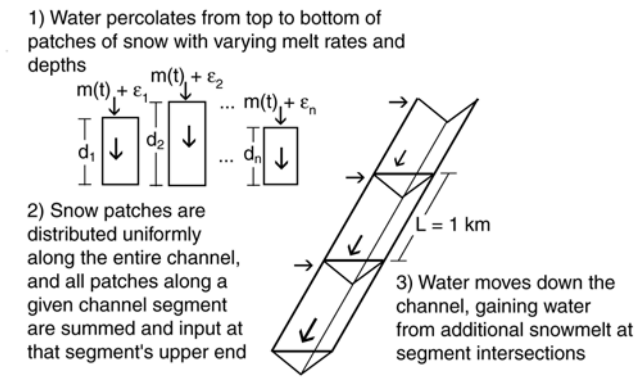

Figure 7. Diagram of the main elements of the VVM.

so the distribution of snow depths within a basin reflects the distribution of elevations. Among nested subbasins of the Merced and Tuolumne Rivers in Yosemite National Park, the standard deviation of elevation increases as basin area, A, raised to the 1/4th power. Therefore an estimate of the increase of heterogeneity of snow depth with basin size is $\sigma \propto A^{1/4}$. The average elevation of snow pillows examined here is 2355 m with a standard deviation of 345.6 m, which is similar to that observed for a subbasin area of 300 km^2. Although the snow pillows span an area of approximately 20,000 km^2, their standard deviation is smaller than that for the larger subbasins in Yosemite because snow pillows do not monitor the highest peaks or lowest elevations and thus cover a truncated range of elevations. Assuming that the observed snow depth standard deviation of 1 m is representative of a 300 km^2 subbasin, a first estimate of how snow depth varies with basin scale would be $\sigma \approx \frac{1}{4}A^{1/4}$.

[15] In addition to elevation, snowpack properties vary with differences in slope, aspect, net solar radiation, wind exposure, and vegetation. The ranges of variability of these properties are also commonly greater in large basins than in small ones. Thus snow variability is larger at all scales and increases more with scale than the elevation-only estimate used here.

3. Variable Velocity Model

[16] Past studies of small basins, described in section 1, indicate that travel times through the snowpack can be measured by diurnal streamflow timing. The heterogeneities described in section 2 indicate that travel times through the snowpack can vary widely between different locations in a basin. This section describes a variable velocity model (VVM) to estimate how contributions from heterogeneous snowpacks join to form the downstream (gauged) diurnal cycle in basins of varying size and heterogeneity. The model tests the hypothesis that increasing heterogeneity in snowpack properties results in a slower seasonal evolution of diurnal streamflow timing, while increasing heterogeneity in channel properties has relatively little effect.

[17] The VVM models two main elements of melted water's journey from the snowpack to the stream gauge (Figure 7). The first element is the vertical propagation of meltwater through a snowpack, which captures the asymmetry of the diurnal cycle [*Lundquist and Cayan*, 2002] and the shift in hour of peak flow to earlier in the day as the snow depth decreases. Water propagates independently through patches of snow with different initial depths and melt rates. The melt pulse from the bottom of each snow patch is assumed to translate immediately to the stream, as has been observed in cases where rapid pressure transmission causes outflow to be quickly released from subsurface reserves to the channel [*Martinec et al.*, 1982; *Thorne et al.*, 1998]. Thus the output from adjacent snow patches is summed and directly input to the upper end of the nearest channel grid cell.

[18] The second model component routes water through the channel to the gauge, adding local snowmelt at each channel grid cell as the water moves downstream (Figure 7). The VVM models the combined basin output from differing flow paths. Different flow paths are generated by considering channels of differing lengths and geometries, and contributing snowpacks with different snow depths and melt rates. The VVM is an idealized representation and does not explicitly model hillslope processes, preferred flow paths through the snow [*Kattelmann and Dozier*, 1999; *Williams et al.*, 2000], variations in soil/subsurface properties [*Bengtsson et al.*, 1992; *Gibson et al.*, 1993; *Laudon et al.*, 2004; *Price and Hendrie*, 1983; *Thorne et al.*, 1998], or horizontal water exchanges within the snowpack. Potential errors arising from these exclusions are discussed in section 4c.

3.1. Propagation Through the Snowpack

[19] The snowpack element of the model describes vertical propagation of meltwater through an unsaturated snowpack. Following *Dunne et al.* [1976], the water moves with a speed proportional to its flux, such that

$$\frac{\partial z}{\partial t} = Km(t)^{\frac{a-1}{a}} \tag{1}$$

where z is the vertical distance from the top of the snowpack, t is time, and m is the melt flux at the surface in m s^{-1}. Daily melt fluxes are estimated from the snow pillows and distributed over the day as half sinusoids with peaks at solar noon, a shape consistent with the diurnal cycle of solar radiation. The transmissibility

$$K = \frac{a}{\phi_e}\left(\frac{\rho g k_u}{\mu}\right)^{\frac{1}{a}} \tag{2}$$

and is assumed to be constant over the course of a day. The parameters are assigned as follows: a is the permeability, set equal to 3 (based on fieldwork by *Colbeck and Davidson* [1973]); ϕ_e is the effective porosity, set equal to 0.52 (based on observed densities and direct measurements by *Colbeck and Anderson* [1982]); ρ is the density of water at 0°C; g is the gravitational acceleration; k_u is the intrinsic permeability, set equal to 2.2×10^{-9} m^2 (the average value observed by *Colbeck and Anderson* [1982]); and μ is the kinematic viscosity of water at 0°C. With these values, K = 1.4 m$^{1/3}$ s$^{-1/3}$. Larger melt fluxes overtake smaller melt fluxes so that shock waves develop [*Dunne et al.*, 1976; *Singh et al.*, 1997]. Thus the shape and timing of the melt waves leaving the snowpack vary nonlinearly with snow depth and melt rate.

3.2. In-Channel Flow

[20] Meltwater flux from the bottom of the snow propagation model is the input to the second model component.

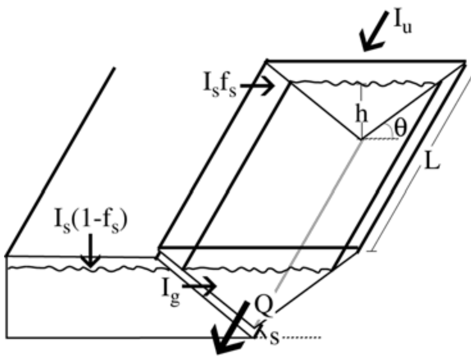

Figure 8. Diagram of the river-routing component of the VVM. I_u is the upstream input, I_s is the local snowmelt input, f_s is the fraction of surface flow, I_g is the groundwater input, L is the length of the channel segment in this grid cell, h is the height of the water column, s is the slope of the channel bottom, θ is the angle of the channel walls, and Q is the output from the channel (which will be I_u to the channel segment immediately downstream).

First the flux is partitioned into surface and subsurface/groundwater components (Figure 8). The surface flow is routed down the nearest channel using the Manning equation (following *Henderson* [1966] and *Kouwen et al.* [1993]) assuming a *V*-shaped cross section with a constant side slope, θ, and time and space varying inundated heights, h. θ is set at 18°, the average side slope observed from a 30 m digital elevation model (DEM) of the Merced and Tuolumne River basins. From the Manning equation, the streamflow velocity, V, for this geometry is

$$V = \frac{1}{n} R^{2/3} \sqrt{s} = \frac{1}{n} \left(\frac{h \cos \theta}{2} \right)^{2/3} \sqrt{s} \tag{3}$$

where n is Manning's roughness coefficient, assumed to be 0.07, a typical value for mountain streams [*Fread*, 1993], R is the hydraulic radius, and s is the longitudinal slope of the channel.

[21] Combining the Manning equation with the channel grid cell's length, L, and the cross-sectional area of the stream, equation (3) can be solved for height variations, such that

$$\frac{\partial h}{\partial t} = \frac{2I \tan \theta}{Lh} - \frac{1}{nL} \left(\frac{h}{2} \right)^{5/3} (\cos \theta)^{2/3} \sqrt{s} \tag{4}$$

where I is the total inflow into the channel grid cell, defined as the sum of local surface meltwater input, $f_s I_s$, groundwater input, I_g, and upstream input, I_u (Figure 8), where I_s is the grid cell snowmelt input, and f_s is the fractional surface runoff, assumed to be 10% based on the relative amplitude of the diurnal cycle in snow-fed streams in the western U.S. [*Lundquist and Cayan*, 2002].

[22] The change in water stored in a surface channel grid cell, S, per unit time, t, is modeled as

$$\begin{aligned}\frac{\partial S}{\partial t} = &\text{ local snowmelt input} + \text{upstream grid cell outflow} \\ &+ \text{groundwater inflow} - \text{outflow downstream.}\end{aligned} \tag{5}$$

Subsurface flow is routed using a simple linear reservoir. The change in water stored in the subsurface grid cell, S_g, is modeled as soil percolation input minus groundwater outflow, Q_g, as

$$\frac{\partial S_g}{\partial t} = I_s(1 - f_s) - Q_g \tag{6}$$

Groundwater storage is linearly related to groundwater outflow such that

$$Q_g = K_g^{-1} S_g, \tag{7}$$

where K_g is a groundwater delay time. In the present application, K_g is set to 2.5 days, the average value measured from the recession slopes of the Merced River at Happy Isles during declining flows in the first half of the melt seasons from 1992 to 2003 [*Lundquist*, 2004]. A variable order solver (MATLAB's ode15s [*Shampine and Reichelt*, 1997]) is used to forward step a finite difference approximation for (4) and calculate discharge and velocity as a function of changing height for each grid cell along the channel.

3.3. Representing Variable Flow Paths Through Channels and Snowpacks

[23] Both components of the model, the snowpack and the channel, are expected to have a wider variety of travel paths and hence increased variation in travel times, as basin scale increases. To test the relative importance of the different contributions, the model was run in three modes: (1) increasing channel variability while holding snowpack properties fixed, (2) increasing snowpack variability while holding channel properties fixed, and (3) increasing variability in both the snowpack and the channel with increasing basin scale.

[24] The time spent traveling along channel flow paths will vary for water parcels originating at different points in the basin, and the range of variation increases with basin scale [*Skøien et al.*, 2003]. Differences in channel travel times are modeled by changing channel lengths and channel configurations. Doubling Manning's roughness coefficient, quadrupling the slope, or reducing the channel length by half all have the same effect on travel time. Thus, from the perspective of travel times, varying channel lengths can be a proxy for variations in other channel properties as well.

[25] First, the changes in travel times with increasing channel lengths were tested by simulating diurnal flow cycles in a hypothetical basin with a linear channel, which was varied from a total length of 1 to 60 km, the range observed in the DEM for the Tuolumne and Merced Rivers. The contributing area, A_i, for a given channel length, L_i, was set in each case to be $A_i = \frac{L_i^2}{3}$ [*Eagleson*, 1970]. Each modeled channel segment was 1 km long, and additional segments were added to make longer channels. In another set of simulations, variability in channel length with basin scale was modeled by having tributaries of length L_i feed into each 1 km long channel segment. Tributary lengths were selected randomly from a normal distribution that varies according to the main channel length L_M, such that tributary lengths have a mean of $\frac{L_M}{2.5}$ and a standard deviation of 50%, which is $\frac{L_M}{5}$, based on the stream order relationships developed by *Horton* [1945] and channel lengths estimated

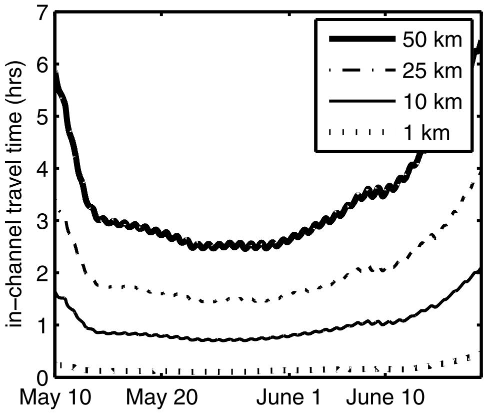

Figure 9. Simulated travel times versus day of year within the stream channel, measured by $\sum_{i=1}^{N} \frac{L_i}{v_i}$.

from the Tuolumne and Merced DEMs. In both sets of simulations, the basin was assumed to be mostly snow covered, without a retreating snow line, throughout the period of analysis, so mean channel length did not vary with time.

[26] To represent variations in snowpack properties, each snow patch was assigned an initial snow depth selected from a normal distribution (the distribution observed by *Elder et al.* [1991]) with a mean and a standard deviation measured from the snow pillows (Figure 6). Imposed melt rates were selected from a distribution with a standard deviation equal to that measured from the snow pillows and varied with location in the modeled catchment to simulate variations due to factors such as elevation, aspect, and vegetation. Location-based melt rate perturbations were held constant throughout the season, so that each location had a constant offset from the temporally varying basin-wide mean, which was calculated each day from all snow pillows where snow was present. The snow depth at each location decreased according to its melt rate. The perturbed snow depths and melt rates were input to the model, and the output was calculated for 200 simulated locations, weighted equally so that each patch represented 1/200th of the total basin area. These snowmelt outputs were distributed uniformly along each stream channel, both main and tributary, and the output from all snowpacks adjacent to each channel segment were summed and input to the channel as illustrated in Figure 7. For example, in a 10 km long channel, each 1 km segment received input from 20 snow patches. This technique represents the mixing that must occur from melt pulses originating from snow patches of various depths and with varying solar forcing and can be thought to represent subchannel segment variability.

4. Model Results and Analysis

[27] In these simulations, increasing snowpack heterogeneity decreased the variation of diurnal streamflow timing as the snowmelt season progressed. Increasing heterogeneity of channel properties did not affect the seasonal evolution of diurnal streamflow timing.

4.1. Results: Channel Heterogeneities

[28] The effects of channel travel times on the timing of daily peak flows were explored by varying channel lengths with one fixed random set of snowpack properties for all runs. The collection of snowpacks was generated from a normal distribution with the mean and standard deviation observed at the snow pillows. Because longer channels drain larger basin areas, both discharge and channel velocities increase downstream. The net effect is that in-channel travel time increases less and less with each additional channel segment (Figure 9). Near the peak of the melt season (30 May), a water parcel spends 1 hour traveling along a 10 km channel but only 3 hours traveling along a channel five times as long (Figure 9). Thus, even very long channels introduce only a few hours of delay to the daily hour of peak flow (Figure 10) and do not change the overall pattern of streamflow timing. In addition to short channel travel times, melt pulses originate all along the channel, so that only a fraction of the total signal travels the entire channel length.

[29] Input from side channels of varying lengths changed diurnal cycle timing very little. The total time delay for each model simulation with side channel input was less than 1 hour more than the time delay for the same main channel length with no side channel input. This delay was longest (about 1 hour) for longer (50 to 60 km) channels and shortest (almost indistinguishable) for shorter (1 to 10 km) channels. The seasonal shift toward streamflow peaks arriving earlier each day was the same for all cases.

4.2. Results: Snowpack Heterogeneities

[30] To isolate the effects of snowpack heterogeneity, the channel parameters were held fixed at a length of 9 km and a slope of 0.06, much like the Rafferty Creek Basin in the Tuolumne River Watershed (a basin explored in further

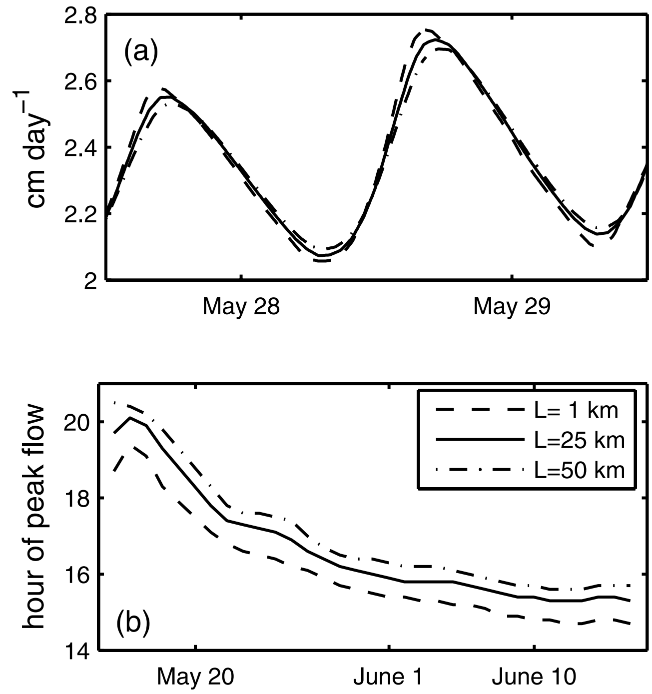

Figure 10. Streamflow timing as a function of changing channel length and basin size, holding snowpack variation constant. (a) Discharge versus time on 2 days for channels with lengths of 1, 25, and 50 km. (b) Hour of peak flow versus day of year for the same three channels.

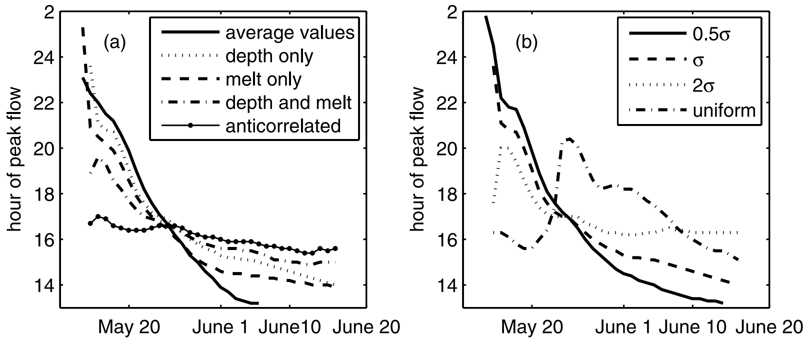

Figure 11. Model simulations of hour of peak flow versus time for 2003 with different variations in model input parameters. (a) Hours of peak flow when snow depth and melt rate are varied independently and then simultaneously. Dashed line labeled "depth and melt" represents independent variations, and the line with dots represents anticorrelated variations. (b) Hours of peak flow when snow depth is varied, with depths chosen from different distributions, with half and double the standard deviation observed between snow pillows, such that $\sigma = \pm 50\%$, $2\sigma = \pm 100\%$, and $0.5\sigma = \pm 25\%$. The uniform distribution simulation randomly selected snow depths from a uniform distribution between the minimum and maximum values (0.25 and 4 m) observed at the snow pillow stations.

detail by *Lundquist* [2004]). As illustrated above, the choice of these channel parameters has very little effect on the evolution of streamflow timing during the melt season.

[31] When the 2003 mean snow depth and melt rate was applied uniformly to all snowpacks in the model, peak flow times decreased about 10 hours during 20 days of melting (Figure 11a). However, when heterogeneous variations were introduced, the diurnal timing changed less. As more and more heterogeneity was applied, diurnal timing changed less and less over the course of the season, until the time of peak flow varied by less than 1 hr during the melt season. The increased heterogeneity could be due to varying snow depth, varying melt rate, varying both depth and melt independently, or varying both in an anticorrelated manner (Figure 11). Heterogeneous initial snow depths resulted in temporally varying snow covered areas during a simulation. When initial snow depth variations were selected from a normal distribution with the standard deviation observed at the snow pillows in 2003 ($\sigma = \pm 1$ m), and melt rates did not vary spatially, the time to peak discharge decreased by 5 hours over 20 days (Figure 11a).

[32] Varying melt rates ($\sigma = \pm 1.5$ cm d^{-1}) but not initial snow depths resulted in a 6 hr change in flow timing. Higher melt rates resulted in larger water fluxes and faster percolation rates, and thus dominated the diurnal timings observed in streams. Hence the travel time delays in the simulation with melt rate heterogeneities were always less than the delays in the simulation with snow depth variations alone. When both snow depths and melt rates were spatially heterogeneous in the model simulation, the combined timing effect was greater than that from varying either property alone, resulting in a net change of peak flows coming 3 hours earlier over the course of the season. In general, though, snow depths increase with altitude, and melt rates decrease with altitude. Thus perturbations in snow depths and melt rates may be anticorrelated, such that deeper snowpacks tend to experience lower melt rates. In this model simulation, the tendency for shallower snowpacks to run out of snow first was exacerbated, and the deep snowpacks left at the end had slower melt rates and longer travel times. When anticorrelated heterogeneities were imposed, streamflow timing varied less than 1 hour during the melt season (Figure 11a).

[33] Several previous studies have indicated that, in snowmelt runoff models, accurate representation of snow depth and SWE heterogeneities at the start of the melt season is more important than capturing spatial variability of melt rates [*Anderton et al.*, 2002; *Dunn and Colohan*, 1999; *Luce et al.*, 1998; *Hartman et al.*, 1999]. The VVM shows that increasing the initial variability of snow depth alone can result in more consistent diurnal streamflow timing even when melt rates do not vary spatially (Figure 11b). Using average melt rates for 2003, snow depths were specified with half, and then double, the observed standard deviation between snow pillows. Greater heterogeneity in snow depths yielded more consistent timing of peak flows. When initial depths were specified randomly, but with only half of the observed standard deviation, the time to peak flow decreased by 8 hours over 20 days, a time shift only 2 hours less than that for the uniform depth simulation described above. When initial depths varied by double the observed standard deviation, the time to peak flow decreased less than 4 hours over the simulation period. When snow depths were selected at random from a uniform distribution between the smallest and largest observed values (25 and 400 cm), the times of peak flows were nearly equal at the start and end of the simulation, with later peak flows in the middle.

[34] These results indicate that, in order to reproduce the observed behavior in diurnal cycle timing, either snow depth and melt rate perturbations must be negatively correlated (Figure 11a) or the actual standard deviation between initial snow depths must be larger than that measured by available snow pillows (Figure 11b). Both of these possibilities are supported by observations, of negatively correlated depth and melt and of large standard deviations in snow properties [*Anderton et al.*, 2002].

[35] As discussed in section 2 and section 3c, variability in snowpack properties can be related to both basin area and channel length ($\sigma \approx \frac{1}{4}A^{1/4}$ and $A = \frac{L^2}{3}$), such that $\sigma \approx 0.19\sqrt{L}$. Thus a standard deviation of half that measured at the snow pillows, $\sigma = 0.5$, would correspond to a 7 km long

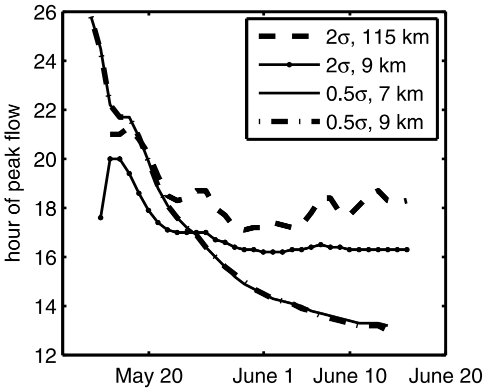

Figure 12. Combined effects of increasing snow depth heterogeneity with increasing channel lengths. Hours of peak flow for 9 km channel simulations are identical to those plotted in Figure 11b.

basin, and a standard deviation double that of the snow pillows, σ = 2, would correspond to a 115 km long basin. The model was run in both of these configurations to test the combined effects of increasing heterogeneity and basin scale (Figure 12).

[36] For the small basin, the timing in the 7 km basin was almost identical to that generated in the 9 km basin simulation discussed above. For the large basin, the time of peak flow was delayed 1 to 2 hours longer in the 115 km channel than in the 9 km channel. However, the overall trend in peak flow timing over the season, with peak flows arriving 3 hours earlier at the end of the simulation than the beginning, was the same for both channel lengths. These results suggest that the degree of variability in snowpack properties is more important than channel length in determining how the time of daily peak streamflow changes over the melt season.

4.3. Why Does Heterogeneity Reduce Seasonal Timing Changes?

[37] Three factors associated with snowpack heterogeneity work to produce the observed and modeled results. Changes in snow covered area during the melt season act to slow the effective basin-averaged decrease in snow depth and act to reduce the change in diurnal streamflow timing as the season progresses. Faster than average melt rates result in faster overall travel times near the start of the season, offsetting the time delays introduced by deep snowpacks at that time. Finally, early in the season, travel times in deep snowpacks can exceed 24 hours and contribute to early afternoon peaks the following day, resulting in aliasing. All three of these factors were captured by the VVM by simply incorporating heterogeneous snow depths and melt rates.

4.3.1. Slower Effective Decrease in Snow Depth

[38] At first glance, one might expect that the snowpack all over a basin gets thinner as the melt season progresses, so that the overall travel time decreases regardless of basin scale or heterogeneity. It might appear that some delicate balancing act, manipulating the precise combinations of melt rates and snowpack thicknesses through time, would be required to avoid this basin response. To the contrary, several aspects of the snowpack heterogeneity combine naturally to prevent the expected travel time decreases, provided the heterogeneity is broad enough.

[39] Only those sites where snow is both present and melting contribute to streamflow and thus delays in streamflow timing. Therefore, as snow covered area decreases, previously shallow snow sites no longer contribute to the effective mean snow depth. Because shallow snowpacks disappear first, each time snow runs out at a site, the sites with above-average snow depths make up a greater part of the remaining average. To illustrate, imagine two very simple "basins," both with average snow depth, d (Figure 13). In one basin (Figure 13a), the snow is distributed uniformly, and in the second (Figure 13b), the snow depth varies such that half the basin has a depth of $0.5d$ and half has a depth of $1.5d$. Now melt half the snow, $0.5d$, in both basins. In the uniform basin (Figure 13a), the depth has decreased to $0.5d$. In the heterogeneous basin (Figure 13b), the average depth, where snow is present, would be d (again). The difference between the two basins occurs because the snow covered area changes in the heterogeneous basin, and the snow-free zone no longer contributes to the average depth.

[40] By the same principle, the average snow depth at 47 snow pillow stations in 2003, for snow pillows that are still snow covered at each time, decreases more slowly than the snow depth at an individual station (Figure 14). The decrease in snow depth was about -10 cm d^{-1} at every individual station, but the net change in mean snowpack depth, considering only locations with snowpack left, was only -5 cm d^{-1}, half that at the individual stations. This effect is greatest when the largest ranges of snow depths exist because snow-free areas are added most incrementally and constantly as melt progresses.

[41] Another way to explain how snowpack heterogeneity contributes to a slower decrease in snow depths and evolution of diurnal flow timing is through differences in the capture of solar radiation to melt snow. Radiation on snow surfaces produces melt. For a given snow water amount, snow distributed uniformly across a basin will melt

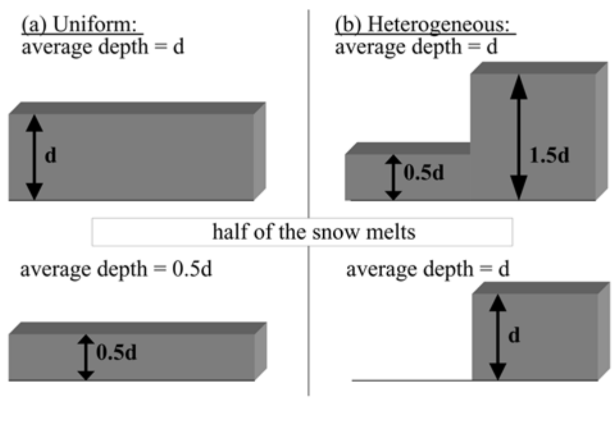

Figure 13. Comparison of two simple "basins," both with average snow depth, d. (a) Snow distributed uniformly; (b) snow depth varied. Half the snow melts in both cases. In the uniform case (Figure 13a) the depth has decreased by half. In the heterogeneous case (Figure 13b) the average depth stays the same because the snow-free zone no longer contributes to streamflow timing.

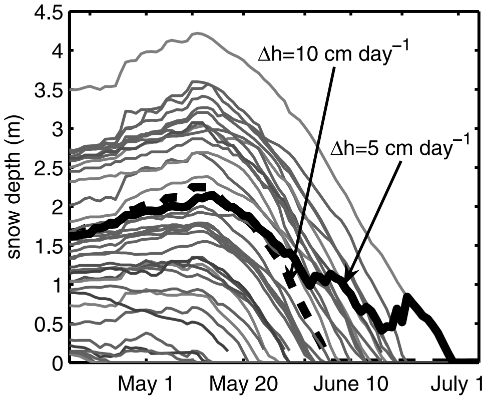

Figure 14. Snow depth versus time at 47 snow pillow stations in 2003. At an individual station (thick dashed line), snow depth decreases about 10 cm d^{-1}. The average snow depth (thick solid line) decreases 5 cm d^{-1}, at half the rate at an individual station.

most rapidly because it has the maximum possible surface area to absorb radiation. However, if the entire snowpack were piled deeply in one corner of the basin, a much smaller surface area would be exposed to radiation, and melt would progress more gradually. Thus shrinking snow covered areas, resulting from initial snowpack heterogeneity, reduce overall melt rates and net changes in snow depths within basins.

4.3.2. Melt Rate Dominance

[42] Areas with larger melt rates produce larger fluxes of meltwater and thus play a disproportionate role in determining the streamflow timing downstream. Because of the nonlinearity of unsaturated flow through the snowpack, the daily snowmelt pulses from areas with greater melt rates also arrive much earlier than the pulses from areas with lower melt rates. Because travel times through the snowpack in areas with large melt rates are short, presumably throughout the melt season, the contributions to streamflow timing from areas with high melt rates have less capacity to change through the season than would contributions from areas with average or slower melt rates. A basin with heterogeneous melt rates would have a tendency for earlier arrival times overall than a basin with uniform melt rates, and would have less room for the times to shorten than would the uniform basin. Thus heterogeneity of melt rates, which involves some areas having faster melt rates than the average, results in travel times that erode less during the course of a melt season than would the travel times in a basin with a uniform melt rate equal to the mean.

[43] Additionally, areas with greater than average melt rates tend to run out of snow earlier, decreasing the snow covered area and reducing the net decrease in snow depth (as described in section 4.3.1). After areas with rapid melt disappear, more water originates from areas with slower than average melt rates, increasing net travel times late in the season. Although all melt rates increase over the course of the season, melt heterogeneity results in net travel times that are shorter than the mean early in the season and longer than the mean later in the season. When combined with the opposing trends introduced by decreasing snow depths, melt rate heterogeneity establishes a smaller range of variation over the whole season.

4.3.3. Yesterday's Melt

[44] Initially, discharge from deep snowpacks can peak more than 24 hours after the snowmelt began its journey (Figure 15a). Thus streamflow contributions from the deepest packs can arrive a few hours after the following day's afternoon snowmelt maximum, aliasing with the next day's output from very thin snowpacks and creating an artificially early mean travel time from a basin. After melt rates increase and snowpacks thin sufficiently (Figure 15b), discharges from nearly all snowpacks peak less than 24 hours after the snowmelt maximum, so little aliasing occurs. Without yesterday's melt being added to the early afternoon peaks, the measured average basin travel time is longer. For example, a 350 cm snowpack peaks at 1900 local time with a melt rate of 0.04 cm hr^{-1} (Figure 15a) and 2100 local time with a melt rate of 0.16 cm hr^{-1} (Figure 15b) and has the effect of shifting diurnal streamflow timing later even while the travel time in the snowpack is significantly less. This shift of diurnal peak flow to later that occurs when aliasing ends is most apparent when snow depths are chosen from a uniform distribution (4 hour added delay following 20 May, Figure 11b), because in this case, the deepest snow depths are weighted equally with mean snow depths. In all cases where snowpacks are normally distributed, deep snowpacks cover a much smaller fraction of the total area, and the effect of aliasing is smaller.

[45] To further illustrate how aliasing affects net streamflow timing, the melt propagation model was run with five different melt rates (0.04–0.20 cm hr^{-1} average daily melt) at sixteen different snow depths (25–400 cm, the total range observed by snow pillows at the start of melt in 2003). The sum of the output from the 16 snow depths contained small,

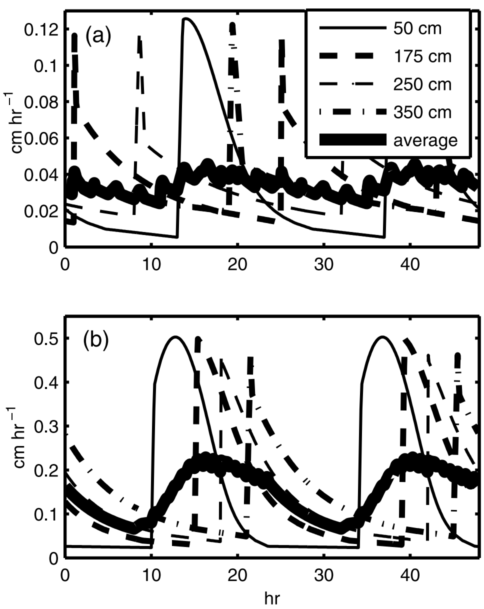

Figure 15. Discharge, in terms of meltwater flux, versus time from the bottom of snowpacks of four different depths and for the average of all depths (thick solid line) between 25 and 400 cm for (a) early in the melt season when melt rates are low (0.04 cm hr^{-1}) and (b) later in the melt season after melt rates increase (0.16 cm hr^{-1}).

jagged spikes from the arrivals of the various individual flow peaks (Figure 16a). As the melt rate increased, the individual spikes arrived closer together, corresponding to the reduced range of flow timing shown in Figure 15. The time of diurnal peak flow for the average remained close to 16:30 for all melt rates, in spite of the shift to earlier peak timing experienced by each individual snowpack. The travel time spent in the snowpack for each of the five melt rates (Figure 16b) increased nonlinearly with snow depth, due to the development of a shock front. Because of shock front development, the range of travel times as a function of melt rate is much greater for deeper snowpacks. Even though travel times decreased at all snow depths as melt rates increased, the resulting net travel time changed less than 1 hr. In the simulations and the real world, the snow depths decreased at the same time as melt rates increased. With declining snow depths, aliasing and nonlinear changes in travel time with shock front formation alone are not enough to hold net travel times constant. The two effects discussed in sections 4.3.1 and 4.3.2, which depend primarily on snow covered area decreasing through the melt season, must also play a role.

4.4. Model Sensitivity

[46] To test the model's sensitivity to the chosen parameters, the VVM was run while varying each of its parameters within ranges reported in the literature. Within these ranges, in the snowpack propagation component, only the intrinsic permeability (k_u) had a significant effect on streamflow timing. The model was run with k_u values varying from 3.0×10^{-10} to 3.0×10^{-8} m^2 [*Bengtsson*, 1981; *Colbeck and Anderson*, 1982; *Dunne et al.*, 1976; *Sommerfeld and Rocchio*, 1993] and yielded early melt season travel times varying by as much as 24 hours. However, the sum of the discharge generated by all of these simulations resulted in travel times that differed from those generated by the average k_u value by less than 0.1 hr throughout the melt season. This indicates that spatial heterogeneity in k_u need not influence net basin streamflow timing, unlike heterogeneities of snowpack depths and melt rates, which yielded timing effects that did not average out linearly. Temporal changes in k_u affected how streamflow timing progressed during the melt season. When k_u was decreased linearly, during a 40 day model run, from the maximum to the minimum values reported in the literature, the hour of peak streamflow stayed constant through the melt season. However, the reported permeabilities come from very different locations with different snowpack properties, and no evidence suggests that k_u could change this widely in one snowpack in one season. *Colbeck and Anderson* [1982] repeatedly measured k_u at the Central Sierra Snow Lab. When k_u was decreased linearly from their maximum and minimum values (4.0 to 1.4×10^{-9} m^2), the hour of peak streamflow came 6 hours earlier at the end of the simulation than at the beginning, compared to the 8 hour change observed for a constant permeability. However, temporal trends in k_u should not vary with basin scale and would not be expected to contribute to the scale-based differences in streamflow timing. For simplicity and to save on computational time, only the average value of k_u was used in VVM.

[47] The influences of seasonal variations in snowpack density were also tested. At Tuolumne Meadows, during the 2003 melt season, density increased from 350 to 600 kg m^{-3} over 30 days. *Sommerfeld and Rocchio* [1993] modeled k_u as a function of snow density, $k_u = 1.096 \times 10^{-8} e^{-9.57\rho_s}$, where ρ_s is snow density and k_u decreases as density increases. The influences of seasonal changes in density alone and changes in permeability and density together were both tested. The model run with permeability and density change together simulated streamflow peaks half an hour earlier at the start of the melt season and half an hour later at the end of the simulation than in the simulation with constant values. The effect of changing density alone was similar but varied less than half an hour from the constant case. The changes in diurnal cycle timing were small because the greater densities occurred when SWE was small and travel times through the snow were negligible. For simplicity, density was assumed to be constant in VVM.

[48] Several processes, including travel along preferential flow paths through the snow and travel across the hillslope from the snowpack to the stream, were not modeled explicitly. Macropores and flow fingers can transport water to the channel before the snowpack is completely ripe, and water can move downslope along ice layers parallel to the strata during the first few days of snowmelt, completely

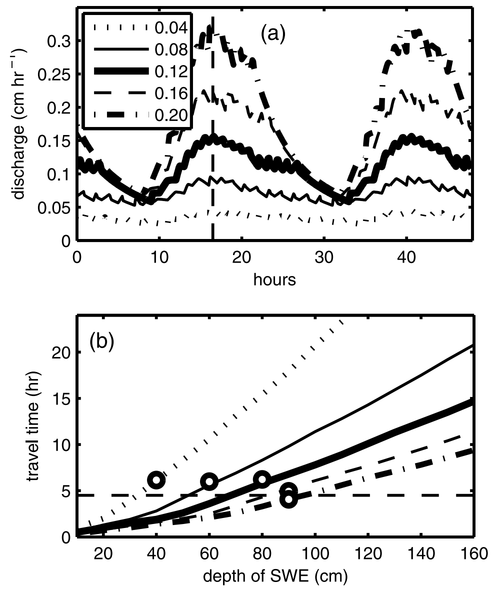

Figure 16. (a) Discharge/meltwater flux versus time as a function of melt rate (cm hr^{-1}). The line plotted for each melt rate is the sum of output from 16 snow depths (25–400 cm), where small spikes indicate the individual peaks. Notice that as the melt rate increases, the individual spikes become closer together, resulting in a longer period of smooth decline in the daily cycle. The time of diurnal peak for the average remains close to 1630 for all melt rates, in spite of the shift to earlier peak timing experienced by each individual snow depth. (b) The travel time spent in the snowpack as a function of snow depth for each of the five melt rates. The circles identify the average travel time for all 16 snow depths, including the effects of aliasing (i.e., a delay of 28 hours would contribute to an average delay of 4 hours). The depth at which the shock front occurs can be identified by the kink in each line, where the velocity slows and travel time increases more rapidly with depth.

bypassing the lower snowpack [*Kattelmann and Dozier*, 1999]. Thus water flow may be faster than equations (1) and (2) predict. If these fast flow paths are more pronounced early in the season, that is, if initial melt input to the stream channel comes mostly from rapid flow fingers and downslope flows while later melts instead travel through the entire snowpack depth, the shifts of peak flows toward earlier in the day as the season progresses would be reduced and could potentially be reversed. Thus, under these circumstances, these preferential pathways could act to make a small, more homogeneous basin, appear more like a large, heterogeneous basin. On the other hand, if the flow fingers and fast travel paths become more developed as the season progresses, discharge would exit the snowpack faster later in the season, due both to the snow's decreasing depth and its increasing permeability. This trend would increase the trend of peak flow to shift to earlier in the day. Under these circumstances, large, heterogeneous basins would begin to act more like small basins.

[49] Meltwater moves quickly from the hillslope to the stream during wet periods when the groundwater table rises to the surface [*Price and Hendrie*, 1983] and in situations with fast subsurface flow paths, such as pipes [*Bengtsson et al.*, 1992; *Gibson et al.*, 1993] or fractures [*Thorne et al.*, 1998]. In much of the Sierra Nevada, soils are thin, unfrozen, and moist, and the water table is presumed to rise near the surface quickly during the early melt season. However, in other settings, soil properties may play a larger role in diurnal streamflow timing. Several studies have observed that overland flow is common in regions with frozen soils [*Bengtsson et al.*, 1992; *Gibson et al.*, 1993]. Thus transport from the snow to the stream may be faster early in the season, when soils are frozen, than later, when more meltwater passes through unfrozen soil layers. This process of increasing travel times could offset the decreasing travel times through the snowpack and could make a small basin with frozen soils exhibit more uniform streamflow timing. Because frozen soils are more likely to occur at higher altitudes, i.e., smaller basins, this process cannot explain the observed basin-scale-dependent change in diurnal streamflow characteristics. In situations where the groundwater table lies below the surface, the rate at which water is discharged to the stream increases with both soil moisture content and the height of the groundwater table [*Laudon et al.*, 2004]. As the melt season progresses, both soil moisture and groundwater levels rise, which would lead to shorter travel times later in the season. This process would enhance the effect of the thinning snowpack and could make a large, heterogeneous basin act more like a small basin. Again, this cannot explain changes in streamflow timing with basin scale. Flow paths through both the snowpack and the hillslope are highly variable in basins and add a component of variability in snowpack travel times that was not modeled here.

[50] Observations of the hour of peak flow in basins throughout the western U. S. [*Lundquist and Cayan*, 2002] suggest that the average travel time from peak melt to peak discharge each day is short and can be accounted for by snow and channel propagation times alone. Therefore propagation times through hillslopes can be approximated as perturbations adding extra time in the snowpack or extra time in the stream channel. Travel times spent in preferential flow paths can also be considered part of the uncertainty in effective snow depth and snowpack propagation times.

[51] In the channel propagation component, only changing channel slope and Manning's roughness coefficient affect streamflow timing by more than ±0.5 hour. In long channel reaches, these variations can offset travel times by several hours. For a channel reach of 10 km or less, however, the offsets are less than ±0.5 hour. In general, slope decreases down channel, so variable slope was modeled as $s_i = s_{ref} \left(\frac{A_i}{A_{ref}}\right)^{-0.6}$ [*Flint*, 1974], where s_i is the slope of channel segment i that drains an upstream area A_i. Rafferty Creek, with a slope of 0.06 and length of 9 km provided the reference parameters. The more gentle slopes at the lower end of a 60 km long channel delayed streamflow peaks by less than 1 hour compared to a channel of the same length with a uniform slope of 0.06. Therefore changes in channel slope with basin scale are unlikely to affect the observed changes in diurnal timing patterns.

5. Conclusions

[52] Previous studies [*Bengtsson*, 1981; *Braun and Slaymaker*, 1981; *Caine*, 1992; *Jordan*, 1983a; *Kobayashi and Motoyama*, 1985] have suggested that streamflow timing might indicate the average snow depth in a basin. The current study uses a physically based model to demonstrate that basin-averaged diurnal streamflow timing is strongly affected by variability in snow depths and melt rates. Mean snowpack properties only determine diurnal streamflow timing in small basins with limited variations in snow depths and melt rates. In these small basins, the hour of daily peak flow generally starts near midnight and then shifts earlier in the day as snow depths and travel times decrease.

[53] When a basin spans larger areas and/or wider ranges of elevations, variabilities of snow depths and melt rates also increase. Summing the outflow from areas with differing snow properties results in remarkably consistent streamflow timing, with little or no variation over the first half of the melt season or between years. This result occurs because the heterogeneity affects the decrease of snow covered areas, resulting in a slower decrease in the average depth of snow in snow covered areas. Heterogeneity also introduces early season aliasing of flow arrival times and allows areas with the fastest melt rates to dominate net timing. These three effects combine to offset the decreases in travel time due to decreasing mean snow depths, resulting in the observed remarkably small seasonal shifts in snowmelt travel times in large, heterogeneous basins. Of these three effects, the first, changing snow covered area, is the most important, as increased variability in snow depth alone can recreate observations. Thus most models that assume 100% SCA throughout the melt period will not do well in recreating observed hourly streamflow timing. Patchy snow cover, which is typically found throughout the Sierra Nevada during the melt season, must be included in a representative model.

[54] The ideas presented here provide ways to learn about snow and basin properties in remote, previously unmonitored basins. Pressure sensors recording stream stage are small, inexpensive, and easy to deploy in remote mountain

areas. Developing rating curves for discharge magnitudes in remote areas is labor-intensive and time-consuming, but precise information about streamflow timing can be gleaned with almost no additional effort. Diurnal timing in small streams, typically with areas less than 30 km^2, provides information about average snow depths and water reserves throughout the melt season. This information could potentially be used to forecast water supply. Timing in larger rivers reveals the degree of heterogeneity within a basin and may provide indications of how many small basins should be monitored to represent variations in snow properties. Timing in many larger rivers is remarkably consistent between years, and this information can be used by hydroelectric power plants to predict the best hours of operation. Current hourly discharge/stage information is already available at most USGS gauges and can be examined and used by operators and forecasters in upcoming melt seasons.

[55] **Acknowledgments.** The authors thank Brad Werner, Dan Cayan, Jeff Dozier, Martyn Clark, Editor Brian Berkowitz, and two anonymous reviewers for comments and suggestions on the manuscript. Brian Huggett and Jim Roche provided field support of the 2002 and 2003 Yosemite observations. Al Leydecker and the UCSB Snow Research Group provided data from the Marble Fork of the Kaweah River, and Frank Gehrke and the California Snow Surveys provided snow sensor and snow survey data. Funding was provided by the Canon National Parks Foundation, the California Institute for Telecommunications and Information Technology, the United States Geological Survey, the NOAA Office of Global Programs through the California Application Program, the NSF ROADNet, and the California Energy Commission.

References

Adams, W. P. (1976), Areal differentiation of snow cover in east central Ontario, *Water Resour. Res.*, *12*, 1226–1234.
Akan, A. O. (1984), Simulation of runoff from snow-covered hillslopes, *Water Resour. Res.*, *20*, 707–713.
Anderton, S. P., S. M. White, and B. Alvera (2002), Micro-scale spatial variability and the timing of snow melt runoff in a high mountain catchment, *J. Hydrol.*, *268*, 158–176.
Bengtsson, L. (1981), Snowmelt generated run-off from small areas as a daily transient process, *Geophysica*, *17*, 109–121.
Bengtsson, L., P. Seuna, A. Lepisto, and R. K. Saxena (1992), Particle movement of melt water in a subdrained agricultural basin, *J. Hydrol.*, *135*, 383–398.
Blöschl, G., and M. Sivapalan (1995), Scale issues in hydrological modeling: A review, *Hydrol. Processes*, *9*, 251–290.
Braun, L. N., and H. O. Slaymaker (1981), Effect of scale on complexity of snowmelt systems, *Nord. Hydrol.*, *12*, 235–246.
Caine, N. (1992), Modulation of the diurnal streamflow response by the seasonal snowcover of an alpine basin, *J. Hydrol.*, *137*, 245–260.
Colbeck, S. C. (1972), A theory of water percolation in snow, *J. Glaciol.*, *11*(63), 369–385.
Colbeck, S. C., and E. A. Anderson (1982), The permeability of a melting snow cover, *Water Resour. Res.*, *18*, 904–908.
Colbeck, S. C., and G. Davidson (1973), Water percolation through homogeneous snow, in *Proceedings, International Symposia on the Role of Snow and Ice in Hydrology, Banff, Canada, Sept. 1972*, vol. 1, pp. 242–257, United Nations Educ., Sci., and Cultural Organ., Geneva, Switzerland.
Davar, K. S. (1970), Peak flow—Snowmelt events, in *Handbook on the Principles of Hydrology*, edited by D. M. Gray, pp. 9.1–9.25, Water Inf. Cent., Inc., Port Washington, N. Y.
Dunn, S. M., and R. J. E. Colohan (1999), Developing the snow component of a distributed hydrological model, a step-wise approach based on multi-objective analysis, *J. Hydrol.*, *223*, 1–16.
Dunne, T., A. G. Price, and S. C. Colbeck (1976), The generation of runoff from subarctic snowpacks, *Water Resour. Res.*, *12*, 677–685.
Eagleson, (1970), *Dynamic Hydrology*, 662 pp., McGraw-Hill, New York.
Elder, K., J. Dozier, and J. Michaelsen (1991), Snow accumulation and distribution in an alpine watershed, *Water Resour. Res.*, *27*, 1541–1552.
Erxleben, J., K. Elder, and R. Davis (2002), Comparison of spatial interpolation methods for estimating snow distribution in the Colorado Rocky Mountains, *Hydrol. Processes*, *16*, 3627–3649.
Flint, J. J. (1974), Stream gradient as a function of order, magnitude, and discharge, *Water Resour. Res.*, *10*, 969–973.
Fread, D. L. (1993), Flow routing, in *Handbook of Hydrology*, edited by D. R. Maidment, pp. 10.1–10.36, McGraw-Hill, New York.
Gibson, J. J., T. W. D. Edwards, and T. D. Prowse (1993), Runoff generation in a high boreal wetland in northern Canada, *Nord. Hydrol.*, *24*, 213–234.
Giorgi, F., and R. Avissar (1997), Representation of heterogeneity effects in Earth system modeling: Experience from land surface modeling, *Rev. Geophys.*, *35*, 413–438.
Hartman, M. D., J. S. Baron, R. B. Lammers, D. W. Clime, L. E. Band, G. E. Liston, and C. Tague (1999), Simulations of snow distribution and hydrology in a mountain basin, *Water Resour. Res.*, *17*, 295–304.
Henderson, F. M. (1966), *Open Channel Flow*, 522 pp., Macmillan, New York.
Horton, R. E. (1945), Erosional development of streams and their drainage basins: Hydrophysical approach to quantitative morphology, *Bull. Geol. Soc. Am.*, *56*, 275–370.
Jordan, P. (1983a), Meltwater movement in a deep snowpack: 1. Field observations, *Water Resour. Res.*, *19*, 971–978.
Jordan, P. (1983b), Meltwater movement in a deep snowpack: 2. Simulation model, *Water Resour. Res.*, *19*, 979–985.
Kattelmann, R., and J. Dozier (1999), Observations of snowpack ripening in the Sierra Nevada, California, U.S.A., *J. Glaciol.*, *45*, 409–416.
Kobayashi, D., and H. Motoyama (1985), Effect of snow cover on time lag of runoff from a watershed, *Ann. Glaciol.*, *6*, 123–125.
Kouwen, N., E. D. Soulis, A. Petroniro, J. Donald, and R. A. Harrington (1993), Grouping response units for distributed hydrologic modeling, *J. Water Resour. Plann. Manage.*, *119*(3), 289–305.
Laudon, H., J. Seibert, S. Kohler, and K. Bishop (2004), Hydrological flow paths during snowmelt: Congruence between hydrometric measurements and oxygen 18 in meltwater, soil water, and runoff, *Water Resour. Res.*, *40*, W03102, doi:10.1029/2003WR002455.
Liston, G. E. (1999), Interrelationships among snow distribution, snowmelt, and snow cover depletion, implications for atmospheric, hydrologic and ecologic modeling, *J. Appl. Meteorol.*, *38*, 1474–1487.
Logan, L. (1973), Basin-wide water equivalent estimation from snowpack depth measurements, in *Role of Snow and Ice in Hydrology*, *IAHS AIHS Publ.*, *107*, 864–884.
Luce, C. H., D. G. Tarboton, and K. R. Cooley (1998), The influence of the spatial distribution of snow on basin-averaged snowmelt, *Hydrol. Processes*, *12*, 1671–1683.
Luce, C. H., D. G. Tarboton, and K. R. Cooley (1999), Sub-grid parameterization of snow distribution for an energy and mass balance snow cover model, *Hydrol. Processes*, *13*, 1921–1933.
Lundquist, J. D. (2004), The pulse of the mountains: Diurnal cycles in western streamflow, Ph.D. thesis, Univ. of Calif., San Diego, La Jolla, Calif.
Lundquist, J. D., and D. Cayan (2002), Seasonal and spatial patterns in diurnal cycles in streamflow in the western United States, *J. Hydrometeorol.*, *3*, 591–603.
Lundquist, J., D. Cayan, and M. Dettinger (2004), Spring onset in the Sierra Nevada: When is snowmelt independent of elevation?, *J. Hydrometeorol.*, *5*, 325–340.
Martinec, J. (1987), Importance and effects of seasonal snow cover, in *Large Scale Effects of Seasonal Snow Cover, Proceedings of the Vancouver Symposium*, *IAHS Publ.*, *166*, 107–120.
Martinec, J., H. Oeschger, U. Schotterer, and U. Siegenthaler (1982), Snowmelt and groundwater storage in an Alpine basin, in *Hydrological Aspects of Alpine and High Mountain Areas, Proceedings of the Exeter Symposium*, *IAHS Publ.*, *138*, 169–175.
Price, A. G., and L. K. Hendrie (1983), Water motion in a deciduous forest during snowmelt, *J. Hydrol.*, *64*, 339–356.
Rickenmann, D. (1994), An alternative equation for the mean velocity in gravel-bed rivers and mountain torrents, in *Proceedings of the National Conference on Hydraulic Engineering*, pp. 672–676, Am. Soc. of Civ. Eng., Reston, Va.
Shampine, L. F., and M. W. Reichelt (1997), The MATLAB ODE Suite, *SIAM J. Sci. Comput.*, *18*, 1–22.
Shook, K., and D. M. Gray (1997), Synthesizing shallow seasonal snow covers, *Water Resour. Res.*, *33*(3), 419–426.
Singh, P., and V. P. Singh (2001), *Snow and Glacier Hydrology*, 742 pp., Springer, New York.
Singh, V. P., L. Bengtsson, and G. Westerstrom (1997), Kinematic wave modeling of vertical movement of snowmelt water through a snowpack, *Hydrol. Processes*, *11*, 149–167.

Skøien, J. O., G. Blöschl, and A. W. Western (2003), Characteristic space scales and timescales in hydrology, *Water Resour. Res.*, *39*(10), 1304, doi:10.1029/2002WR001736.

Sommerfeld, R. A., and J. E. Rocchio (1993), Permeability measurements on new and equitemperature snow, *Water Resour. Res.*, *29*, 2485–2490.

Thorne, G. A., J. Laporte, and D. Clarke (1998), The effects of frozen soils on groundwater recharge and discharge in granitic rock terrain of the Canadian Shield, *Nord. Hydrol.*, *29*, 371–384.

U.S. Army Corps of Engineers (1956), *Snow Hydrology, Summary Report on the Snow Investigations*, 437 pp., North Pac. Div., Portland, Oregon.

Williams, M. W., R. Sommerfeld, S. Massman, and M. Rikkers (1999), Correlation lengths of meltwater flow through ripe snowpacks, Colorado Front Range, USA, *Hydrol. Processes*, *13*, 1807–1826.

Williams, M. W., M. Rikkers, and W. T. Pfeffer (2000), Ice columns and frozen rills in a warm snowpack, Green Lakes Valley, Colorado, USA, *Nord. Hydrol.*, *31*, 169–186.

Woo, M., and H. O. Slaymaker (1975), Alpine streamflow response to variable snowpack thickness and extent, *Geograf. Ann.*, *57*, 201–212.

M. D. Dettinger, U.S. Geological Survey, La Jolla, CA 92093, USA.

J. D. Lundquist, CIRES, Climate Diagnostics Center, University of Colorado, 216 UCB, Boulder, CO 80309-0216, USA. (jessica.lundquist@noaa.gov)